

## Supplementary Materials for

### **A physics-based earthquake simulator replicates seismic hazard statistics across California**

Bruce E. Shaw\*, Kevin R. Milner, Edward H. Field, Keith Richards-Dinger, Jacquelyn J. Gilchrist, James H. Dieterich, Thomas H. Jordan

\*Corresponding author. Email: shaw@ldeo.columbia.edu

Published 22 August 2018, *Sci. Adv.* **4**, eaau0688 (2018)  
DOI: 10.1126/sciadv.aau0688

#### **This PDF file includes:**

- Fig. S1. Map of difference in recurrence intervals in the earthquake simulator compared with UCERF3.
- Fig. S2. Parameter sensitivity study.
- Fig. S3. Parameter sensitivity study.
- Fig. S4. Parameter sensitivity example showing the spatial structure of changes in hazard.
- Fig. S5. Parameter sensitivity example showing the spatial structure of changes in hazard relative to UCERF3.
- Fig. S6. Weak magnitude dependence of GMMs.
- References (25–29)

# Supplementary Materials

## Differences in rupture sets

### Spatial differences in recurrence intervals

In the main body of the text, in Fig. 1a, we compared recurrence intervals in the simulator with UCERF3 for large  $M7+$  events. Here we look into this in further detail, looking at the spatial aspects of the difference. Figure S-1 shows maps of the differences in recurrence rates, ratios of the rates in RSQSim relative to UCERF3, for  $M7+$ , and at a lower magnitude threshold  $M6.5+$ . Comparing fig. S1a and S1b, we see complementarity of how faults are choosing to slip, with faults showing an excess of large  $M7+$  events tending to show a dearth of  $M6.5+$  events, and vice versa. Thus the linkage of faults into moderate or larger events impacts the recurrence interval differences.

Two other notable recurrence interval differences are at the ends of long faults, and how separated faults might be linking up. Differences at the ends of long faults, most easily seen in the offshore borderlands faults in Southern California, the southwesternmost faults in the figure, show up for the following reason. In the case of UCERF3, slip rates are targeted to match a relatively constant rate along strike up to the fault ends. In the simulator case, in contrast, we used loading conditions which lead to stressing rates which are more constant towards the ends of faults. This leads to higher rates of moderate sized events in UCERF3 at the fault ends trying to fill in the more constant slip rates relative to RSQSim, which develops fault slip rates more tapered at the ends. This is an epistemic uncertainty which we could remove by using either more tapered slip in UCERF3, or more constant slip in RSQSim. But seeing the differences which arise are useful in illustrating the origin of the differences between the models, and the broader epistemic uncertainties we end up exploring by having different types of models in dialogue on the problem.

The second area of focus is illustrated in the northeastern California slow moving faults. Here, the rules used in UCERF3 allowed faults less than 5 km separation to link up, while faults

farther apart do not (2, 25). This was based on sparse historical earthquake surface rupture data (26) and individual rupture simulations (27), though multicycle simulators have suggested a more probabilistic approach would be better (28). Here, we see the simulator is allowing faults to link up into longer length ruptures than UCERF3 is accounting for, bridging gaps not considered in UCERF3. This is occurring despite the fact that the simulator only considers static stress interactions, and dynamic stress interactions would encourage even larger gaps to be bridged.

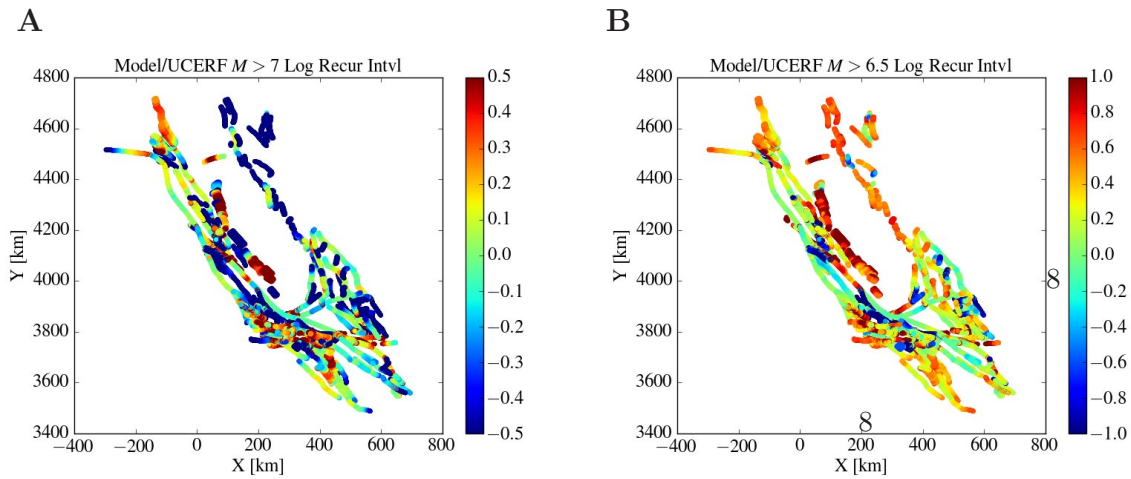


Fig. S1. Map of difference in recurrence intervals in the earthquake simulator compared with UCERF3. (A) Map of log ratio of recurrence intervals for  $M \geq 7$ . Color scale is in  $\log_{10}$  units. (B) Map of log ratio of recurrence intervals for  $M \geq 6.5$ . Color scale is in  $\log_{10}$  units; note it is a wider scale range than in (A), so differences are larger. Note also complementarity of intervals; parts that are bluer in (A) tend to be redder in (B).

## Parameter sensitivity

As mentioned in the main body of the text, a parameter sensitivity study was made using small finite perturbations to frictional parameters around the default ones used. Figure S2 shows the results for perturbing the rate-and-state parameters  $b$  and  $a$ , and the normal stress  $\sigma_n$ . We do not see an overly sensitive response, with perturbations up to  $\pm 25\%$  in the parameters showing a  $< 10\%$  change in the long-term hazard for a range of spectral periods (PGA and  $T = 0.2 - 10s$ ) and annual rates ( $p = 10^{-3} - 10^{-4} yr^{-1}$ ).

We can also look at changes in the hazard relative to UCERF3, to see if the reference set of parameters is a good choice. Figure S3 shows the results for the same set of parameters as in Figure S-2, but now looking at hazard differences relative to UCERF3, rather than the baseline model. We see that while there are some spectral periods and annual rates that have a bit of a trend, favoring a higher or lower parameter value than the reference value, the reference value does a good job in compromising overall, with the lowest peak value difference.

While there is not an overly sensitive response to parameters, there are systematics to the response, as a map view of the differences illustrates. Figure S4 shows how changing the  $b$  friction parameter to values lower and higher than the reference value changes the near field and far field hazard differently.

Maps of PSA(1) 1 second spectral acceleration shaking hazard in earthquake simulator compared with UCERF3 hazard model, and plots of differences, Figure S5 shows how changing the  $b$  friction parameter to values lower and higher than the reference value compares to relative to UCERF3. Because the differences with respect to UCERF3 are much larger than the difference in the model (note the scale bar in fig. S4 is much smaller than the scale bar in this figure), the differences here are much more subtle, and not so easy to see.

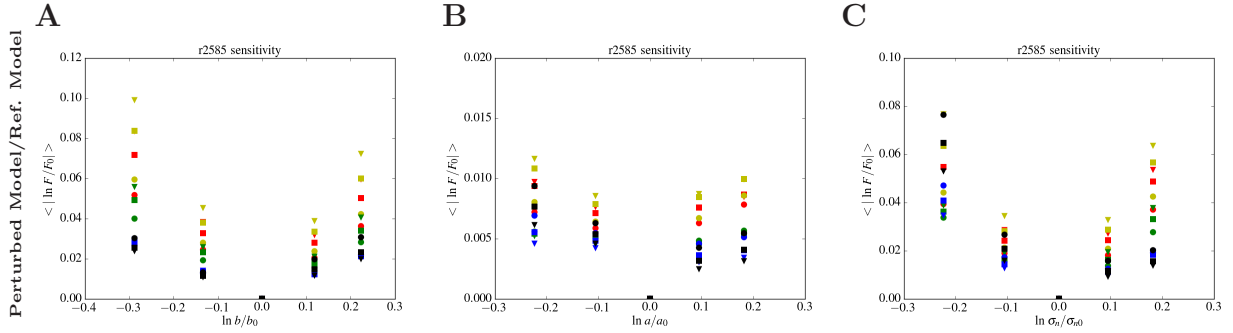


Fig. S2. Parameter sensitivity study. Changes in hazard in model for small finite parameters changes. Horizontal axis is natural log change in parameter relative to reference value. Vertical axis is mean absolute natural log ratio of perturbed model hazard relative to reference model hazard (Thus  $F$  is perturbed model, and  $F_0$  here is reference model). Colors correspond with different spectral periods, with, as in figures in main body of text, PGA (red), to  $T = 0.2s$  (yellow),  $T = 1s$  (green),  $T = 5s$  (blue), and  $T = 10s$  (black). Different symbol types correspond with different annual rates, with  $p = 10^{-3}yr^{-1}$  being a triangle,  $p = 4 * 10^{-4}yr^{-1}$  being a square, and  $p = 10^{-4}yr^{-1}$  being a circle, Note that the vertical scales are different in each case, corresponding with differences in relative parameter sensitivities. **(A)**  $b$  friction parameter. Reference value is  $b = .008$  . **(B)**  $a$  friction parameter. Reference value is  $a = .001$  . **(C)**  $\sigma_n$  normal stress parameter. Reference value is  $\sigma_n = 100 MPa$  .

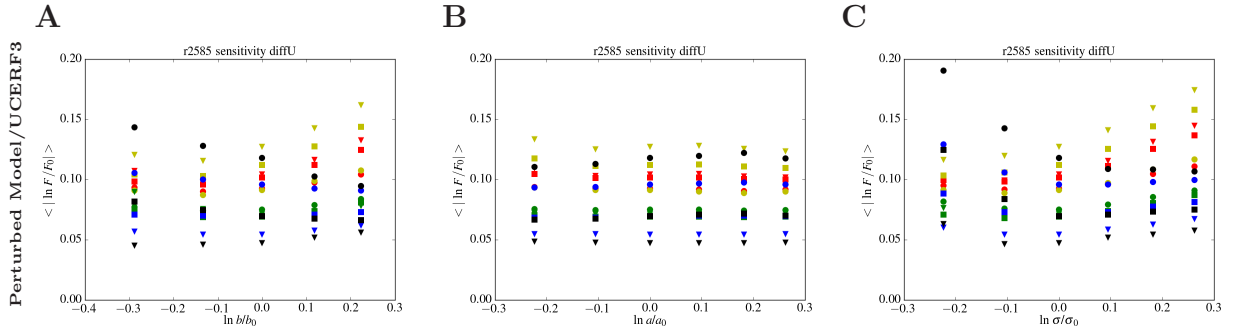


Fig. S3. Parameter sensitivity study. Changes in hazard in model relative to UCERF3 for small finite parameters changes. Horizontal axis is natural log change in parameter relative to reference value. Vertical axis is mean absolute natural log ratio of perturbed model hazard relative to UCERF3 model hazard. (Thus  $F$  is perturbed model, and  $F_0$  here is UCERF3 model). Colors correspond with different spectral periods, with, as in figures in main body of text, PGA (red), to  $T = 0.2s$  (yellow),  $T = 1s$  (green),  $T = 5s$  (blue), and  $T = 10s$  (black). Different symbol types correspond with different annual rates, with  $p = 10^{-3}yr^{-1}$  being a triangle,  $p = 4 * 10^{-4}yr^{-1}$  being a square, and  $p = 10^{-4}yr^{-1}$  being a circle, **(A)**  $b$  friction parameter. Reference value is  $b = .008$  . **(A)**  $a$  friction parameter. Reference value is  $a = .001$  . **(A)**  $\sigma_n$  normal stress parameter. Reference value is  $\sigma_n = 100 MPa$  .

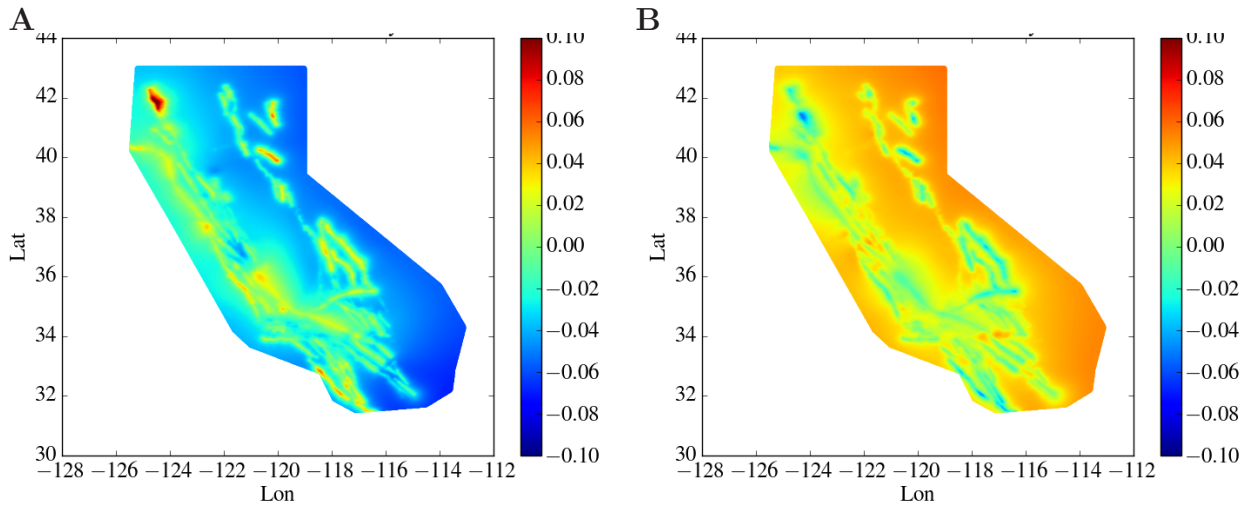


Fig. S4. Parameter sensitivity example showing the spatial structure of changes in hazard. This shows maps of  $\ln$  hazard ratio for perturbed friction relative to reference friction. Here we show the hazard ratio for  $PSA(T)$  with  $T = 10s$  and  $p = 10^{-4} yr^{-1}$  and changes in the friction parameter  $b$ . **(A)** Hazard for  $b = .006$  relative to  $b = .008$ . **(B)** Hazard for  $b = .010$  relative to  $b = .008$ .

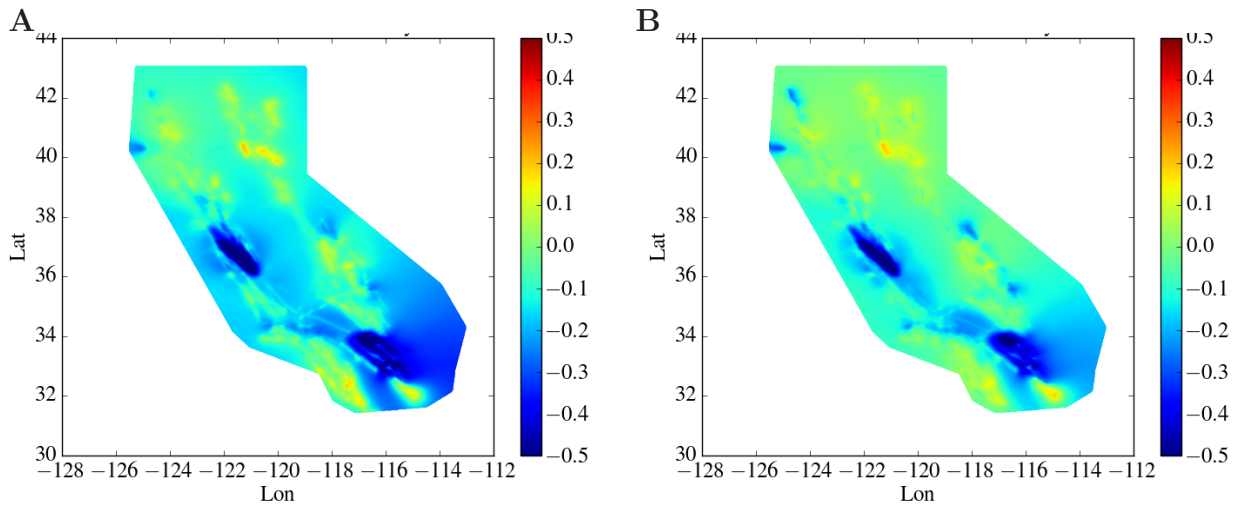


Fig. S5. Parameter sensitivity example showing the spatial structure of changes in hazard relative to UCERF3. These are the same perturbations as in fig. S4, except now they are examined with respect to UCERF3 rather than a reference simulator model. Because the differences with respect to UCERF3 are much larger than the difference in the model (note the scale bar in fig. S4), the differences here are much more subtle, and not so easy to see. Here we show the hazard ratio for  $PSA(T)$  with  $T = 10s$  and  $p = 10^{-4} yr^{-1}$  and changes in the friction parameter  $b$ . **(A)** Hazard for  $b = .006$  relative to UCERF3. **(B)** Hazard for  $b = .010$  relative to UCERF3.

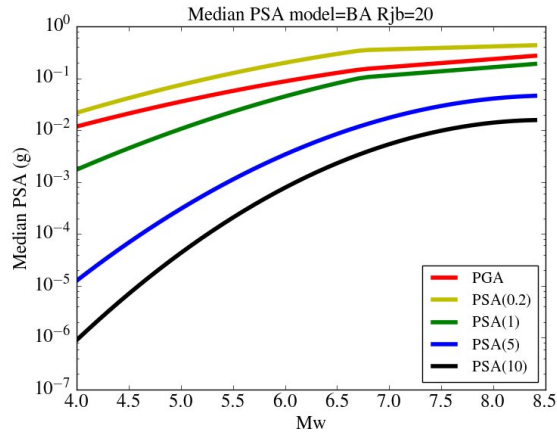


Fig. S6. Weak magnitude dependence of Ground Motion Models. Magnitude dependence of GMM at different spectral periods. Model is by (29). Curves are for a distance of  $20\text{km}$  from fault. Different curves are for different spectral periods, shown with PGA (red), to  $T = 0.2\text{s}$  (yellow),  $T = 1\text{s}$  (green),  $T = 5\text{s}$  (blue), and  $T = 10\text{s}$  (black). Note weak magnitude dependence at large magnitudes ( $M > 6.5$ ) for the short period curves, but then more significant magnitude dependence for the  $T = 5$  and  $T = 10$  curves.

## Mapping simulator ruptures onto UCERF3 fault subsections

As noted in the body of the paper, to focus attention on the differences in the rupture sets, rather than the details of the fault model, we mapped simulator ruptures onto the UCERF3 fault subsections and then calculated shaking with GMMs relative to the fault subsections. Because distance to the rupture is an important parameter in estimating shaking, and simulator ruptures can be quite complex, with sometimes distant triggered elements, we found it useful to introduce a rupture area criteria in mapping the complex simulator ruptures onto the UCERF3 subsections. We used a minimum fractional area cutoff to determine whether a fault subsection broke in a rupture, with a fractional area  $f_A = 0.2$  used in the results presented in the main body of the paper. We checked that the results were insensitive to this parameter choice for a broad range of reasonable values. In particular, changing the  $f_A$  fractional area mapping cutoff by a factor of 2 higher or lower than the default 0.2 value changed mean absolute natural log ratios by less than 1%.

## Ground motion model magnitude insensitivity

At large magnitudes, ground motion models show relatively low magnitude sensitivity. This is especially true at high frequencies (21). Figure S6 illustrates an example of a GMM magnitude dependence in different spectral bands at a given distance from a rupture. Longer spectral periods are seen to have more but still relatively weak magnitude dependence.